Safe Policy Design for Controlling Epidemic Spreading under Heterogeneous Testing Capabilities

Pol Mestres Jorge Cortés

***Abstract*— This paper studies a model that captures epidemic spreading in a population with heterogeneous testing capabilities. The detection of the disease is faster in a subpopulation because of access to better testing capabilities, whereas another subpopulation relies on standard testing to confirm positive cases once individual have manifested symptoms. This model is a particular case of a recently proposed vectorized SIR model, for which we characterize various invariance properties and the stability properties of its set of equilibria. We leverage these analytical results to design social distancing policies that guarantee that the impact of the pandemic satisfies certain specifications, namely, that the total capacity of the healthcare system does not get overburdened and that the total number of infections throughout the pandemic remains below a threshold. Simulations illustrate the extent to which higher testing capabilities allow for more lenient social distancing policies.**

I. Introduction

The spread of COVID-19 across the world and its disruptive implications on the health and well-being of millions of humans has sparked interest in having reliable and accurate models for the spread of a disease in a population. Possessing these models is critical for government authorities, which since the beginning of the pandemic have tried to implement non-pharmaceutical interventions (NPIs) that mitigate the medical, social and economic impacts of the pandemic. An alternative to NPIs to contain the spread is the use of asymptomatic testing mechanisms. In certain situations, COVID-19 leads to pneumonia and severe respiratory complications, in which case patients are sent to Intensive Care Units (ICUs). It is thus critical to keep the number of infections under a certain threshold, that depends on the ICU beds that the population has at their disposal. In this paper we study how a COVID-19-like disease spreads in a population with different testing mechanisms and design the optimal level of NPIs that guarantee that certain safety constraints.

Literature Review: Models for the spread of an epidemic have a long history starting as early as the 18th century [1]. Recently, since the beginning of the COVID-19 pandemic several models tailored to the spread of this disease have been proposed. By using a model that recognizes the fact that only a portion of the infected population is actually symptomatic, [2] studies the early spread of COVID-19 in Italy. The work in [3] introduces a novel model with susceptible (S), infected (I), diagnosed (D), ailing (A), recognized (R), threatened (T), healed (H) and extinct (E) individuals that also takes into account the important feature of COVID-19 that a part of the infections come from asymptomatic but infected individuals. The extent to which COVID-19 can be controlled by the authorities by using data from rapid daily tests has also been studied [4]. The model proposed in [6] is the one most closely related to our work. It generalizes most of the proposed models for COVID-19-like infections, and proposes a novel characterization of the reproduction number as the gain matrix of an appropriately defined linear system. However, the set of equilibria of the newly proposed model is characterized, but their stability properties are not studied. A critical idea that has been explored in the context of COVID-19 is *flattening the curve*, i.e., implementing control policies that guarantee that the fraction of infected/hospitalized remains below a predefined threshold. This is formulated as an optimal control problem in [7], and [8] employs an MPC approach. A recent line of work [9] applies safety-critical control ideas to tackle this issue. Our work is also related to the problem of resource allocation in the context of epidemic spreading [10]. A well-established approach to tackle this problem is using geometric programming [11].

Statement of Contributions: We study[1] dynamical and control properties of a compartmental model that captures the evolution of a disease in interacting subpopulations with different testing capabilities. This model is a particular case of a recently proposed model that generalizes a large class of SIR-like compartmental models. Our first contribution is the derivation of a set of conserved quantities for the general model. Moreover, we show how they can be used to give a novel proof of the transcendental equation satisfied by the asymptotic fraction of the different susceptible compartments. Our second contribution states the relationship between the reproductive number of the model and the stability properties of both the set of equilibria and each of the equi-

This work was supported by NSF Award ECCS-1947050.

P. Mestres and J. Cortés are with the Department of Mechanical and Aerospace Engineering, University of California, San Diego, {pomestre,cortes}@ucsd.edu

[1]Throughout the paper, we denote by $\mathbb{R}$ and $\mathbb{R}_{\geq 0}$ the set of real and non-negative real numbers, and by $\|\cdot\|$ the Euclidean norm in $\mathbb{R}^n$. We use the notation $\mathbf{0}_n$ and $\mathbf{1}_n$ to represent the n-dimensional zero and one vectors, respectively. A matrix $A \in \mathbb{R}^{n+m}$ is *positive*, denoted $A > 0$, (*non-negative*, denoted $A \geq 0$) if all its entries are positive (non-negative). By extension $A < B$ ($A \leq B$) means that $B-A$ is positive (non-negative). The spectral radius $\rho(A)$ of a square matrix A is the largest absolute value of its eigenvalues. We denote by $\lambda_{\max}(A)$ the largest real part of the eigenvalues of A. A matrix of the form $A = sI - B$, with $B \geq 0$ and I the identity matrix, has the Z *sign pattern*. If in addition, $s \geq \rho(B)$, then A is an M*-matrix*. A matrix is *Metzler* if all the off-diagonal components are non-negative. Given a vector $x \in \mathbb{R}^n$, $\mathrm{diag}(x)$ denotes the diagonal matrix with x in its diagonal. A continuous function $\alpha : [0, a) \to [0, \infty)$, $a > 0$, is of class $\mathcal{K}$ if it is strictly increasing and $\alpha(0) = 0$. For $a = \infty$, we refer to it as an *extended* class $\mathcal{K}$ function. A set $\mathcal{U}$ is *positively invariant* under the dynamical system $\dot{x} = f(x)$ if any trajectory with initial condition in $\mathcal{U}$ remains in $\mathcal{U}$ for all time. We use $L_f h$ to denote the Lie derivative of the function h along the vector field f. A dynamical system is positive if the set $\mathbb{R}^n_{\geq 0}$ is positively invariant. A linear system $\dot{x} = Ax$ is positive if and only if A is a Metzler matrix.

librium points in the set for the general model. Our last contribution is the design of a control policy for our model that keeps the maximum fraction of infections below a predefined threshold and the total number of infections throughout the pandemic below another threshold. We achieve the former by using theory on high order control barrier functions and the latter by leveraging the transcendental equation satisfied by the asymptotic fraction of susceptibles. We integrate these two constraints in an optimization problem that is solved online. Simulations with real data from two zip codes in San Diego County illustrate the performance of the proposed approach. For space reasons, all proofs are omitted and will appear elsewhere.

II. Preliminaries

Here we present basic concepts on compartmental epidemiological models and high-order control barrier functions.

A. Compartmental Models in Epidemiology

Compartmental models are a common framework to model the spread of an infection in a population [12]. The population is divided in groups or *compartments* and individuals transition between them at different rates, depending on the specific model. One of the most commonly used compartmental models is the Susceptible-Infected-Recovered (SIR) model, in which susceptible individuals get infected at some constant rate and infected individuals recover at some other constant rate. The addition of an Exposed (E) compartment to model the incubation period in which an individual is infected but asymptomatic yields the also commonly used SEIR model. Multiple variations of these basic models have been proposed, including networked versions [13] and models tailored to the characteristics of COVID-19 [3]. The recently introduced model in [6] generalizes all of the above by proposing a vectorized version of the SIR model which takes the following form,

$$\dot{S} = -\operatorname{diag}(S)TI, \tag{1a}$$

$$\dot{I} = AI + B\operatorname{diag}(S)TI, \tag{1b}$$

$$\dot{R} = C\tilde{A}I. \tag{1c}$$

We will henceforth refer to this model as the *vectorized SIR model*. Here $S \in \mathbb{R}^m_{\geq 0}$, $I \in \mathbb{R}^n_{\geq 0}$, $R \in \mathbb{R}^p_{\geq 0}$ represent the fraction of individuals of the total population in the susceptible, infected or exposed, and recovered or removed compartments respectively. The matrix $T \in \mathbb{R}^{m\times n}$ encodes the rate at which the infected or exposed compartments infect the susceptibles and $B \in \mathbb{R}^{n\times m}$ details how the newly infected or exposed get distributed in the different compartments. The matrix $A \in \mathbb{R}^{n\times n}$ captures the rate of transition between the different infected or exposed compartments, and from those to the recovered or removed. Finally, $C \in \mathbb{R}^{p\times n}$ and $\tilde{A} \in \mathbb{R}^{n\times n}$ encode how the newly recovered or removed get distributed across different compartments (the reason why the term $C\tilde{A}$ is expressed as the product of two different matrices is so that one can impose simple consistency conditions on C and $\tilde{A}$ separately). The conditions that need to be satisfied by those matrices are:

(i) A is stable,
(ii) A is Metzler and $\tilde{A}, B, C, T \geq 0$,
(iii) each of the columns of B and C sum to 1,
(iv) the columns of $A + \tilde{A}$ sum to 0,
(v) all rows of T have at least one strictly positive element.

Intuitively, (i) ensures that the number of infected or exposed individuals converges to zero, (ii) ensures that the state variables remain non-negative and, therefore, physically meaningful, (iii) ensures that the total population is conserved and (iv) ensures that the positive orthant is positively invariant. Finally, (v) guarantees that the fraction of individuals in the susceptible compartments is strictly decreasing as long as there are exposed and infected individuals.

The reproduction number of an epidemic model is the average number of secondary infections generated by an infected individual. It is often useful to have an explicit expression for it, as it is related to the ability of a disease to persist in a population. According to [6, Theorem 3], the reproductive number $\mathcal{R}_0$ for (1) can be expressed as the spectral radius of the matrix $-TA^{-1}B\operatorname{diag}(S_0)$, where S_0 is the initial fraction of susceptibles.

B. High-Order Control Barrier Functions

In this section we review the concept of High-Order Control Barrier Functions (HOCBFs) [14]. Consider a control-affine dynamical system

$$\dot{x} = f(x) + g(x)u, \tag{2}$$

where $x \in \mathbb{R}^n$ and $u \in U \subset \mathbb{R}^q$, with $f : \mathbb{R}^n \to \mathbb{R}^n$ and $g : \mathbb{R}^n \to \mathbb{R}^{n\times q}$ locally Lipschitz. Let $b : \mathbb{R}^n \to \mathbb{R}$ be a function which defines a safe set of the form

$$\mathcal{C} := \{x \in \mathbb{R}^n : b(x) \geq 0\}.$$

We seek to ensure that all system trajectories remain in $\mathcal{C}$ along their evolution, i.e., that $\mathcal{C}$ is positively invariant. Let $m \in \mathbb{Z}_{>0}$ be the relative degree of b (i.e., b has to be differentiated m times along the dynamics (2) before the control u explicitly appears in the expressions). This means that, in order to ensure that the value of b remains positive at all times (i.e., $\mathcal{C}$ is positively invariant), we need to reason with its higher-order derivatives. To do so, given differentiable class $\mathcal{K}$ functions $l_1, l_2, \ldots, l_{m-1}$, define a series of functions $\phi_0, \ldots, \phi_{m-1} : \mathbb{R}^n \to \mathbb{R}$ as follows: $\phi_0 = b$ and

$$\phi_i(x) = L_f\phi_{i-1}(x) + l_i(\phi_{i-1}(x)), \quad i \in \{1, \ldots, m-1\}.$$

We further define sets $\mathcal{C}_1, \ldots, \mathcal{C}_m$ as follows: $\mathcal{C}_1 = \mathcal{C}$ and

$$\mathcal{C}_i = \{x \in \mathbb{R}^n : \phi_{i-1}(x) \geq 0\}, \quad i \in \{2, \ldots, m\}.$$

The function b is a high-order control barrier function (HOCBF) if one can find differentiable, class $\mathcal{K}$ functions $l_1, l_2, \ldots, l_m$ such that, for all $x \in \mathcal{C} \cap \mathcal{C}_2 \cap \ldots \cap \mathcal{C}_m$, there exists $u \in U$ satisfying

$$L_f\phi_{m-1}(x) + L_g\phi_{m-1}(x)u + l_m(\phi_{m-1}(x)) \geq 0. \tag{3}$$

If $m = 1$, this definition corresponds to the notion of Control Barrier Function (CBF). According to [14, Theorem 5], any

Lipschitz continuous controller that satisfies (3) at each $x \in \mathcal{C} \cap \mathcal{C}_2 \cap \ldots \cap \mathcal{C}_m$ renders the set $\mathcal{C} \cap \mathcal{C}_2 \cap \ldots \cap \mathcal{C}_m$ positively invariant for system (2).

III. Problem Statement

Given two subpopulations of individuals forming a larger community, consider the scenario where the detection of the disease is faster in one subpopulation because of access to better testing capabilities (e.g., wastewater detection plants installed in large residential buildings, regular asymptomatic scheduled tests, robust contact tracing protocols), whereas the other subpopulation relies on standard testing to confirm positive cases once individual have manifested symptoms. Susceptible individuals might get infected by being in contact with individuals who either are aware of having the disease or have been exposed to the disease but are still unaware of having it. Once infected, an individual enters an exposed state in which it is infected and infectious but is unaware of it. After some time, the individual becomes aware of being infected, either because it becomes symptomatic or tests positive. If an individual belongs to the subpopulation with higher testing capabilities, it becomes aware of being infected in a shorter time period than individuals belonging to the subpopulation with lower testing capabilities, and it can therefore implement self-isolation and contact tracing protocols earlier to help reduce the spread of the disease. Individuals recover from the disease at the same rate from both subpopulations and never become susceptible again.

Under this scenario, we are interested in studying to what extent the availability of better testing capabilities and the relative size of the population that has access to them impacts the spread of the disease. There is a tradeoff between the cost of deploying such testing capabilities and the societal and economic benefits that result from having them. One could envision, for instance, that such capabilities allow for the implementation of more lenient lockdown measures given that positive cases can be detected more rapidly. We consider the following description of the disease evolution:

$$\begin{aligned}
\frac{ds}{dt} &= -\beta_i si - \beta_e se_1 - \beta_e se_2,\\
\frac{de_1}{dt} &= \sigma\beta_i si + \sigma\beta_e se_1 + \sigma\beta_e se_2 - \alpha_1 e_1,\\
\frac{de_2}{dt} &= (1-\sigma)\beta_i si + (1-\sigma)\beta_e se_1 + (1-\sigma)\beta_e se_2 - \alpha_2 e_2,\\
\frac{di}{dt} &= \alpha_1 e_1 + \alpha_2 e_2 - \gamma i,\\
\frac{dr}{dt} &= \gamma i. \qquad (4)
\end{aligned}$$

The variable s represents the fraction of individuals in the susceptible population. The fraction of infected but unaware (for simplicity, we henceforth refer to those as *exposed*) individuals in the subpopulation with higher (resp., lower) testing capabilities is e_2 (resp., e_1). The fraction of individuals in the population that are infected and aware (for simplicity, we refer to those as *infected*) is i. Finally, r represents the fraction that are recovered (or removed).

The parameters β_i and β_e are the infection rates with which the infected aware and infected unaware, respectively, infect the susceptible population. Given the setup described above, $\beta_i < \beta_e$, i.e., unaware infected infect at a faster rate than aware infected. These rates are determined by the number of interactions between individuals and are therefore tunable as a function of the social distancing policy in place. The recovery rate is γ, with $\frac{1}{\gamma}$ representing the time it takes for an individual to recover from the disease. The parameter α_1 (resp., α_2) represents the inverse of the time individuals spend being infected but unaware of it in the subpopulation with lower (resp., higher) testing capabilities. Since testing capabilities reduce the time spent being unaware of the infection, $\alpha_2 > \alpha_1$. Finally, σ denotes the relative size of the subpopulation with lower testing capabilities to the total population. It remains constant along the trajectories (because the infection rates for both subpopulations are the same). The parameters are assumed to be strictly positive. Note that (4) does not include the presence of disturbances, that could arise from influx or outflux of people from other communities or uncertainties in the model parameters. We hence assume that the population is completely isolated from its surroundings and the model parameters are known.

Interestingly, the model (4) is a particular case of (1). In fact, this is verified by taking $S = s \in \mathbb{R}$, $I = [e_1, e_2, i]^T \in \mathbb{R}^3$, $R = r \in \mathbb{R}$ and

$$A = \begin{bmatrix} -\alpha_1 & 0 & 0 \\ 0 & -\alpha_2 & 0 \\ \alpha_1 & \alpha_2 & -\gamma \end{bmatrix}, \quad \tilde{A} = \begin{bmatrix} 0 & 0 & 0 \\ 0 & 0 & 0 \\ 0 & 0 & \gamma \end{bmatrix}, \qquad (5)$$

$$T = \begin{bmatrix} \beta_e & \beta_e & \beta_i \end{bmatrix}, \quad B = \begin{bmatrix} \sigma \\ 1-\sigma \\ 0 \end{bmatrix}, \quad C = \begin{bmatrix} 1 & 1 & 1 \end{bmatrix}.$$

Our objective is to characterize the dynamical behavior of the proposed model (4). We seek to leverage this knowledge to determine to what extent the availability of better testing capabilities allows to relax social distancing measures while still guaranteeing that the evolution of the epidemics remains within certain predefined bounds (e.g., to ensure hospitals do not get overloaded). As an intermediate goal, and given the observation that (4) is a particular case of (1), we study the stability and invariance properties of the latter. Building on this understanding, we then seek to synthesize in (4) optimal rates β_i and β_e (as a proxy for optimal social distancing policy) guaranteeing that the fraction of infected never surpasses a predefined threshold and the total fraction of individuals that have been infected throughout the pandemic remains below another predefined threshold.

IV. Invariance and Stability Analysis

In this section we study dynamical properties of (1) regarding invariance properties, the identification of conserved quantities, and the stability of invariant sets and equilibria.

A. Invariance Properties and Conserved Quantities

We start by noting that the evolution of R in (1) is entirely driven by the (S, I)-subsystem, so our analysis here focuses on the latter. We start by noting, cf. [6], that the set of equilibria of the (S, I) subsystem is

$$\mathcal{A} = \{(S, 0) \in \mathbb{R}^{n+m}_{\geq 0} \ : \ \mathbf{0}_m \leq S \leq \mathbf{1}_m\}.$$

Since state variables represent fractions of individuals, they have to remain lower bounded by zero and their sum has to be upper bounded by one. The following result establishes that this physically meaningful domain is positively invariant.

Lemma 4.1: (Positively invariant domain): The set $\Omega = \{(S, I) \in \mathbb{R}^{n+m}_{\geq 0} \ : \ \mathbf{1}_n^T S + \mathbf{1}_m^T I \leq 1\}$ is positively invariant.

The following result gives a set of conserved quantities for (1) which help in understanding its dynamic behavior.

Proposition 4.2: (Conserved quantities): Let $F : \mathbb{R}^{n+m+p} \to \mathbb{R}^m$ and $G : \mathbb{R}^{n+m+p} \to \mathbb{R}^p$ be defined by

$$F(S, I, R) = \log S + TA^{-1}BS + TA^{-1}I,$$
$$G(S, I, R) = -C\tilde{A}A^{-1}(BS + I) + R.$$

Then both F and G are constant along the trajectories of (1).

The next result relates the conserved function G with the total population.

Lemma 4.3: (Total population is conserved): Along the trajectories of (1), we have

$$\mathbf{1}_m^T S + \mathbf{1}_n^T I + \mathbf{1}_p^T R = \mathbf{1}_p^T G(S, I, R). \tag{6}$$

In particular, the total population is conserved.

Remark 1: (Interpretation of G): In the case $p = 1$, Lemma 4.3 implies that G is equal to the total population. In network models, G defines the total population in each of the nodes, and therefore its conservation implies that the population in each node is conserved. •

B. Stability Properties of the Continuum of Equilibria

Here we study the stability properties of the set of equilibria, considered as a whole and as individual points. The next result characterizes the global asymptotic stability properties of the set of equilibria, ruling out limit cycles, and its dependence on the reproduction number $\mathcal{R}_0$.

Proposition 4.4: (Stability of the set of equilibria): Under the (S,I)-subsystem dynamics of (1), the equilibrium set $\mathcal{A}$

(i) is globally exponentially stable in the set

$$\{(S, I) \in \Omega \ : \ \rho(-TA^{-1}B\,\mathrm{diag}(S)) < 1\},$$

(ii) is globally asymptotically stable and locally exponentially stable in Ω.

Moreover, every solution of (1) converges to a point in $\mathcal{A}$.

This result illustrates the relevance of the reproduction number $\mathcal{R}_0$, as it defines a threshold between global and local exponential convergence to the equilibrium set. Similarly to S, R is monotonic (because $\tilde{A}$ and C are positive) and upper bounded. Therefore it converges to a certain value R_∞.

The function F in Proposition 4.2 can be used to give an alternative proof to a result from [6, Theorem 4] on the asymptotic ratio of susceptibles. The function G in Proposition 4.2 can similarly be used to give a novel formula for the asymptotic ratio of removed.

Theorem 4.5: (Transcendental equation for asymptotic ratio of susceptibles [6, Theorem 4] and removed): The vector $\Delta = S_\infty / S_0$ satisfies

$$-\log(\Delta) + TA^{-1}I_0 + TA^{-1}B\,\mathrm{diag}(S_0)(\mathbf{1}_m - \Delta) = 0. \tag{7}$$

The asymptotic fraction of recovered is given by $R_\infty = \lim_{t\to\infty} R(t) = R(0) - C\tilde{A}A^{-1}(B(S_0 - S_\infty) + I_0)$.

We next turn our attention to characterizing the asymptotic stability of the individual equilibrium points. The following illustrates how the reproductive number also defines a threshold for the stability of each point in $\mathcal{A}$. Recall that [15] an equilibrium point is *semistable* if it is Lyapunov stable and there exists a neighborhood such that all trajectories starting in the neighborhood converge to a (possibly different) Lyapunov stable equilibrium point.

Proposition 4.6: (Stability properties of the individual equilibrium points): An $(\hat{S}, 0) \in \mathcal{A}$ equilibrium is semistable if $\mathcal{R}_0 < 1$ and unstable if $\mathcal{R}_0 > 1$.

The interpretation of this result in terms of epidemic spreading is as follows. When the initial ratio of infected I_0 is small (e.g., at the beginning of the spread of the disease), the initial condition is close to the equilibrium set $\mathcal{A}$. In this scenario, Proposition 4.6 states that if the reproduction number is less than one, the epidemic remains localized and most of the population is not infected, whereas if the reproduction number is greater than one, the disease spreads across a non-negligible part of the population.

V. Safe Control Policy Design

Here, we leverage the results of Section IV to introduce a control policy that mitigates the impact of the epidemic. For ease of interpretability, we focus on the model (4), albeit the algorithm can be generalized to the more general model (1). We assume a social planner can determine mobility restrictions which in turn affect the values of the infection rates β_e and β_i. We assume the impact of these restrictions on β_e and β_i is proportional, i.e., $\beta_e = \kappa\beta_i$, for some $\kappa > 0$. Hence, effectively there is only one control variable, which we assume is β_e. Moreover we assume β_e is upper and lower bounded by $\bar{\beta}_e > 0$ and $\underline{\beta}_e > 0$ respectively.

A. Safety Constraints

Our first goal is to keep the fraction of infected below a predefined threshold i_{th} at all times. This ensures that the capacity of the healthcare system does not get overburdened. To tackle this safety constraint, we take a CBF approach as in [9] and define the candidate control barrier function $b : \mathbb{R}^4 \to \mathbb{R}$ as $b(s, e_1, e_2, i) = i_{\mathrm{th}} - i$. Note that, when viewed as the control, β_e has relative degree 2 with respect to b. The following result identifies conditions on the parameters to make sure this function is a HOCBF.

Lemma 5.1: (Sufficient conditions for a HOCBF to exist): If $\underline{\beta}_e \geq 0$, $\alpha_2 > \alpha_1$ and

$$\underline{\beta}_e \leq \frac{\alpha_1\gamma i_{\mathrm{th}}}{(1+\kappa)(\alpha_1\sigma + \alpha_2(1-\sigma))}, \tag{8}$$

then b is a HOCBF for (4).

The condition $\alpha_2 > \alpha_1$ follows from the fact that one of the subpopulations has higher testing capabilities, cf. Section III. Regarding the condition (8), note that smaller incubation ($1/\alpha_1$) and recovery ($1/\gamma$) periods, as well as a higher threshold for infected (i_{th}) yield a larger bound on $\underline{\beta}_e$, meaning that more lenient social distancing measures are to

be expected. By the discussion in Section II-B with $m = 2$, Lemma 5.1 implies that the set defined by $\mathcal{C} \cap \mathcal{C}_2$, with

$$\mathcal{C} = \{(s, e_1, e_2, i) \in \Omega \ : \ i \leq i_{\rm th}\},$$
$$\mathcal{C}_2 = \{(s, e_1, e_2, i) \in \Omega \ : \ \gamma i_{\rm th} \geq \alpha_1 e_1 + \alpha_2 e_2\},$$

is positively invariant if we use a Lipschitz continuous controller β_e satisfying $y(i_{\rm th}, \beta_e, s, e_1, e_2, i) \geq 0$ along all points of a trajectory.

Our second goal is to keep the total number of infections throughout the pandemic below certain desired level. This is equivalent to requiring that s_∞ remains above a certain threshold $s_{\rm th}$. Using a control barrier function to tackle this constraint could be problematic since the decreasing nature of s makes the resulting inequality potentially infeasible for all values of β_e. Instead, we leverage (7) to identify the constraint $z(s_{\rm th}, \beta_e, s, e_1, e_2, i) \geq 0$ on β_e, where

$$z(s_{\rm th}, \beta_e, s, e_1, e_2, i) = \log(s) - R_0(\beta_e)s - (\frac{\kappa\beta_e}{\gamma} + \frac{\beta_e}{\alpha_1})e_1$$
$$- (\frac{\kappa\beta_e}{\gamma} + \frac{\beta_e}{\alpha_2})e_2 - \frac{\kappa\beta_e}{\gamma}i + \log(s_{\rm th}) - R_0(\beta_e)s_{\rm th}.$$

In this expression, $R_0(\beta_e) = \frac{\kappa\beta_e}{\gamma} + \sigma\frac{\beta_e}{\alpha_1} + (1-\sigma)\frac{\beta_e}{\alpha_2}$ is the reproduction number for (4).

B. Minimizing Social Costs while Guaranteeing Safety

In this section, we incorporate the two safety constraints discussed in Section V-A in an optimization problem that minimizes the economic and societal costs. In practice, it is not possible to continuously monitor the state and therefore ensure that those constraints are satisfied for all times. Instead, we assume we have access periodic access to the fraction of susceptibles, exposed and infected. Hence, we solve the optimization problem periodically and propagate the dynamics with the corresponding solution. Let T_0 be a pre-specified initial intervention time and $\delta > 0$ the period used to update the social distancing measures. Define $t_j = T_0 + j\delta$, $j \in \{0, \dots, N\}$ as the intervention times where the social distancing measures can be updated. At each of these times, consider the linear program

$$\begin{aligned} \max_{\beta_e \in [\underline{\beta}_e \bar{\beta}_e]} \quad & \beta_e \\ \text{s.t.} \quad & y(i_{\rm th}, \beta_e, s_j, e_{1,j}, e_{2,j}, i_j) \geq 0, \\ & z(s_{\rm th}, \beta_e, s_j, e_{1,j}, e_{2,j}, i_j) \geq 0, \end{aligned} \tag{9}$$

where $s_j, e_{1,j}, e_{2,j}, i_j$ are the values of s, e_1, e_2, i at time t_j, respectively. Algorithm 1 formalizes the iterative procedure to update the social distancing measures.

The following result gives a sufficient condition on the parameters of the model so that the optimization problem remains feasible (and hence Algorithm 1 can be executed) and quantifies the safety error induced by solving the problem periodically instead of continuously.

Proposition 5.2: (Feasibility and maximum unsafety bound): Let $\underline{s}_{\rm th}$ and $\bar{s}_{\rm th}$ be defined by the transcendental equations $z(\underline{s}_{\rm th}, \bar{\beta}_e, s_0, e_{1,0}, e_{2,0}, i_0) = 0$ and $z(\bar{s}_{\rm th}, \underline{\beta}_e, s_0, e_{1,0}, e_{2,0}, i_0) = 0$. Under the conditions in Lemma 5.1, suppose that $\underline{s}_{\rm th} \leq s_{\rm th} \leq \bar{s}_{\rm th}$. Then,

Algorithm 1: Periodic Updates of Social Distancing

Initial conditions: $\{s_0, e_{1,0}, e_{2,0}, i_0\} \in \mathcal{C} \cap \mathcal{C}_2$;
Parameters: T_0, δ, N, γ, α_1, α_2, σ, κ, $\underline{\beta}_e$, $\bar{\beta}_e$;
for $j \in [1, \dots, N]$ **do**
  Solve (9) to obtain optimal $\beta^*_{e,j}$;
  Reset $\beta_e := \beta^*_{e,j}$, $\beta_i := \kappa\beta^*_{e,j}$;
  Run dynamics (1) for $[t_{j-1}, t_j]$;
  $j \leftarrow j + 1$;
end

(i) At every iteration of Algorithm 1, (9) is feasible;
(ii) The inequalities $s(t) \geq s_{\rm th}, \quad i(t) \leq i_{\rm th} + K\delta$ are satisfied for all $t \in [0, (N+1)\delta)$, where

$$K = \frac{1}{\alpha_1\gamma}\big(\alpha_2(\alpha_2 - \alpha_1)L_{e_2} + \bar{\beta}_e L(\alpha_1\sigma + \alpha_2(1-\sigma))\big),$$
$$L = \kappa L_i + L_{e_1} + L_{e_2},$$

and L_{e_1}, L_{e_2} and L_i are Lipschitz constants for e_1, e_2 and i, respectively.

Proposition 5.2(ii) guarantees that if the optimization problem is solved frequently enough, the safety error is kept arbitrarily small. It also ensures that the fraction of infected can be kept below $i^*_{\rm th}$ by taking $i_{\rm th} = i^*_{\rm th} - K\delta$ in Algorithm 1.

VI. Simulations

In this section we illustrate the performance of the proposed Algorithm 1. We use (4) to model the evolution of the pandemic at the University of California, San Diego (UCSD) and its surrounding areas. This is inspired by the observation that, since the start of the 2020-2021 academic year, UCSD implemented an extensive program for early detection of the virus both via wastewater detection plants and massive availability of rapid antigen tests. During the same period of time, the zip codes surrounding UCSD did not take such measures. To fit the model, we use real data of the COVID-19 pandemic in two zip codes: 92093 (UCSD) and 92037 (the rest of La Jolla). The San Diego Open GIS Data Portal[2] provides free access to the accumulated daily total cases of COVID-19 for all zip codes in San Diego County from as early as March 31, 2020 to March 21, 2021. We fit a piecewise constant β_e that changes every 10 days. By considering the typical incubation and recovery periods of COVID-19, as well as the fact that the massive testing capabilities implemented at UCSD reduce the number of days an individual is infected but unaware of it to two, we take α_1, α_2 and γ in (4) to be $1/5$, $1/2$ and $1/10$, respectively. Since the testing plan at UCSD started at September 1st, 2020, we take $\sigma = 1$ up to that point and $\sigma = 0.9$ (approximately the proportion of people in the 92037 zip-code compared to the sum of the 92093 and 92037 zip-codes) onwards. We are able to obtain optimal

[2]The San Diego Open GIS Data Portal is a data warehouse jointly build by the San Diego Association of Governments (SANDAG) and the San Diego Geographic Information Source (SanGIS), providing open access to geographic, transportation, and related datasets in the San Diego region.

values of β_e that fit the data quite accurately and correlate well with the social distancing measures enforced by the state of California. In Figure 1, we compare the hypothetical evolution of the pandemic that would have resulted from applying social distancing policies as given by Algorithm 1 after the intervention time $T_0 = 150$ for different values of σ. We use the data to fit the model up to the intervention time and get an estimate of the state at that point so that we can apply Algorithm 1 onwards. We take $i_{\text{th}} = 3 \times 10^{-3}$ and $s_{\text{th}} = 0.9$. As it can be seen in Figure 1, the real data does not satisfy the safety constraint for the fraction of infected, but the curves obtained by applying Algorithm 1 satisfy both the constraint on the fraction of infected and the fraction of susceptibles. Define the social distancing payoff P as $P = \sum_{j=0}^{350/\delta} \beta_e^j \delta$, with $\delta = 50$ days. For $\sigma = 0, 0.33, 0.66, 1$ we obtain $P = 74.67, 71.44, 68.01, 64.58$, respectively. We see that smaller σ yield a higher P. In other words, by providing access to more testing capabilities to a larger fraction of the population, the social distancing measures can be relaxed while still guaranteeing the same safety specifications.

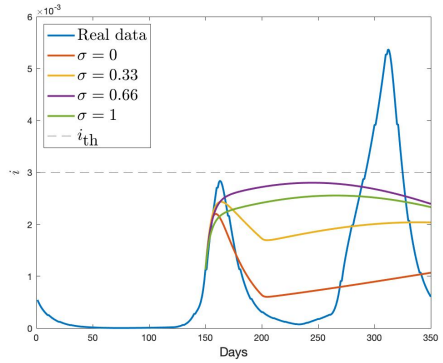

(a)

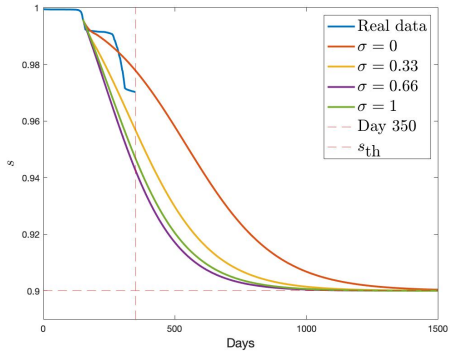

(b)

Fig. 1. Evolution of the fraction of infected (a) and fraction of susceptible (b) under the implementation of Algorithm 1 for different values of σ.

VII. Conclusions

We have introduced a model capturing epidemic spreading in a population with heterogeneous testing capabilities. We have shown this model is a particular case of a recently proposed vectorized SIR model, for which we have identified various conserved quantities and characterized the stability properties of its set of equilibria. We have also introduced a control policy that periodically determines optimal social distancing measures to mitigate the impact of the epidemic. We have given sufficient conditions on the model parameters for the control policy to be well defined and characterized its performance with regards to keeping the fraction of infected at any time and the total fraction of infected individuals below prespecified thresholds. Simulations with COVID-19 epidemic data from UCSD and its surrounding areas suggest that better testing capabilities allow for more lenient social distancing measures while still guaranteeing the same safety constraints. Future work will study the impact of disturbances in the parameters and the dynamics, investigate the opportunistic determination of intervention times to update optimal social distancing measures, and analytically characterize the benefits on better testing capabilities and the fraction of population with access to them on the leniency of the required social distancing measures.

References

[1] K. Dietz and J. Heesterbeek, "Daniel Bernoulli's epidemiological model revisited," *Mathematical Biosciences*, vol. 180, no. 1/2, p. 1, 2002.

[2] G. C. Calafiore, C. Novara, and C. Possieri, "A modified SIR model for the COVID-19 contagion in Italy," in *IEEE Conf. on Decision and Control*, Jeju Island, South Korea, Dec. 2020, pp. 3889–3894.

[3] G. Giordano, F. Blanchini, R. Bruno, P. Colaneri, A. D. Filippo, A. D. Matteo, and M. Colaneri, "Modelling the COVID-19 epidemic and implementation of population-wide interventions in Italy," *Nature Medicine*, vol. 26, no. 6, p. 855–860, Apr 2020.

[4] F. Casella, "Can the COVID-19 epidemic be controllled on the basis of daily test reports?" *IEEE Control Systems Letters*, vol. 5, no. 3, pp. 1079–1084, 2021.

[5] D. Vrabac, M. Shang, B. Butler, J. Pham, R. Stern, and P. E. Pare, "Capturing the effects of transportation on the spread of COVID-19 with a multi-networked SEIR model," *IEEE Control Systems Letters*, vol. 6, pp. 103–108, 2022.

[6] A. Colombo, "The basic reproduction number as a loop gain matrix," *IEEE Control Systems Letters*, 2021.

[7] F. D. Lauro, I. Z. Kiss, D. Rus, and C. D. Santina, "COVID-19 and flattening the curve: A feedback control perspective," *IEEE Control Systems Letters*, vol. 5, no. 4, pp. 1435–1440, 2021.

[8] J. Kohler, L. Schwenkel, A. Koch, J. Berberich, and P. Pauli, "Robust and optimal predictive control of the COVID-19 outbreak," *Annual Reviews in Control*, vol. 51, pp. 525–539, 2021.

[9] T. G. Molnar, A. W. Singletary, G. Orosz, and A. D. Ames, "Safety-critical control of comparmental epidemiological models with measurement delays," *IEEE Control Systems Letters*, vol. 5, no. 5, pp. 1537–1542, 2021.

[10] J. Omic, A. Orda, and P. V. Mieghem, "Protecting against network infections: A game theoretic perspective," *IEEE INFOCOM*, pp. 1485–1493, 2009.

[11] V. M. Preciado, M. Zargham, C. Enyioha, A. Jadbabaie, and G. Pappas, "Optimal resource allocation for network protection: A geometric programming approach," *IEEE Transactions on Control of Network Systems*, vol. 1, no. 1, pp. 99–108, 2014.

[12] F. Brauer, C. Castillo-Chavez, and Z. Feng, *Mathematical Models in Epidemiology*. Springer, 2019.

[13] W. Mei, S. Mohagheghi, S. Zampieri, and F. Bullo, "On the dynamics of deterministic epidemic propagation over networks," *Annual Reviews in Control*, vol. 44, pp. 116–128, 2017.

[14] W. Xiao and C. Belta, "Control barrier functions for systems with high relative degree," in *IEEE Conf. on Decision and Control*, Nice, France, Dec. 2019, pp. 474–479.

[15] R. Goebel, "Results on robust stability and feedback stabilization for systems with a continuum of equilibria," in *IEEE Conf. on Decision and Control*, Los Angeles, CA, USA, 2014, pp. 2282–2286.